

See discussions, stats, and author profiles for this publication at: <https://www.researchgate.net/publication/234847628>

Vibrationally resolved photoelectron imaging of gold hydride cluster anions: AuH⁻ and Au₂H⁻

ARTICLE in THE JOURNAL OF CHEMICAL PHYSICS · JULY 2010

Impact Factor: 2.95 · DOI: 10.1063/1.3456373 · Source: PubMed

CITATIONS

13

READS

76

7 AUTHORS, INCLUDING:



Zhengbo Qin

Anhui Normal University

27 PUBLICATIONS 108 CITATIONS

SEE PROFILE



Hua Xie

Chinese Academy of Sciences

26 PUBLICATIONS 107 CITATIONS

SEE PROFILE



Zichao Tang

Chinese Academy of Sciences

65 PUBLICATIONS 512 CITATIONS

SEE PROFILE



Hong-Jun Fan

Dalian Institute of Chemical Physics

89 PUBLICATIONS 1,721 CITATIONS

SEE PROFILE

Vibrationally resolved photoelectron imaging of gold hydride cluster anions: AuH^- and Au_2H^-

Xia Wu, Zhengbo Qin, Hua Xie, Ran Cong, Xiaohu Wu, Zichao Tang,^{a),b)} and Hongjun Fan^{a),c)}

State Key Laboratory of Molecular Reaction Dynamics, Dalian Institute of Chemical Physics, Chinese Academy of Sciences, Dalian 116023, People's Republic of China

(Received 29 March 2010; accepted 2 June 2010; published online 23 July 2010)

Photoelectron spectra and angular distributions in photodetachment of gold hydride anions AuH^- and Au_2H^- have been obtained using photoelectron velocity-map imaging. Both the images exhibit vibrationally resolved ground state transitions. The adiabatic electron affinities of AuH and Au_2H are measured to be 0.758(20) and 3.437(3) eV, respectively. Franck–Condon analyses of the AuH spectra determined that the equilibrium bond length of the ground state of AuH^- is 1.597(6) Å. The photoelectron images of Au_2H^- show a vibrational progression of 148(4) cm^{-1} assigned to the Au–Au stretching mode at the ground state. *Ab initio* calculation results are in excellent agreement with the experimental results. For the ground state of Au_2H , a new bent Au–Au–H structure with the angle of 131° is suggested. Moreover, energy-dependent photoelectron anisotropy parameters are also reported and discussed. © 2010 American Institute of Physics. [doi:10.1063/1.3456373]

I. INTRODUCTION

Gold hydrides serve as important intermediates in several gold-catalyzed reactions.¹ Studies of the gold hydride clusters are important to understand the adsorption of hydrogen onto metal surfaces and to unveil the origin of the unusual chemical activities of Au. Furthermore, gold hydrides can be used as prototypical test cases to study relativistic effects. Thus, gold hydrides have been the subject of many computational and spectroscopic investigations for decades. Recently, several theoretical and experimental works have demonstrated that the chemistry of gold has significant resemblance to that of the hydrogen atom.^{2,3} Geometric structures of a H atom attached to the small Au clusters have been tackled by theoretical studies.⁴ Several experimental studies on gold hydride clusters have also been reported.^{3–8} Notably, PES spectra for a series of small gold hydride clusters accompanied with density functional theory (DFT) calculations have demonstrated that the spectra of bare Au_{n+1}^- and Au_nH^- clusters for $n > 2$ with the same total number of atoms exhibit a surprising similarity.^{3,4}

The small gold hydrides, AuH and Au_2H , serve as excellent examples of profound effects of relativity.^{9,10} Since the first theoretical study was done by Pyykkö and co-worker,¹¹ extensive accurate relativistic configuration interaction calculations have been performed on AuH .⁹ Several rotational spectra of AuH were reported experimentally.^{8,12,13} For example, Andrews and co-worker⁵ detected infrared spectra for AuH , associated with a fundamental frequency at 2226.6 cm^{-1} . Photoelectron spectra of AuH^- and Au_2H^- obtained with a conventional negative ion time-of-flight (TOF)

photoelectron spectrometer have been reported.^{3,4,7} The photoelectron spectrum of AuH^- indicates that the vertical detachment energy (VDE) is 0.6 ± 0.2 eV.³ For Au_2H^- , only the Au–H vibrational frequency of 2050(100) cm^{-1} was obtained from a well-resolved photoelectron spectrum.⁷ Obviously, the paucity of resolved features in the photoelectron spectra greatly obscure additional chemical information. It prompted us to carry out a careful reinvestigation of the photodetachment of gold hydrides using photoelectron velocity-map imaging (VMI), which is a powerful experimental tool for investigating the electronic properties and dynamics of negative ions in the gas phase, yielding both the photoelectron spectrum and the photoelectron angular distribution (PAD) simultaneously.¹⁴ The analysis of photoelectron spectrum allows the determination of the electron affinity (EA) and vibrational frequencies and provides direct insights into the electronic structures of the parent anions. PADs carry the information of the orbitals where the electrons emerge.

In this work, we report the photoelectron VMI results of AuH^- and Au_2H^- . The photoelectron spectra and PADs have been derived from the velocity-map images. In each spectrum, we observed the vibrationally resolved ground state transition, yielding substantially improved spectroscopic constants. The comparison of electronic structure calculations with the experimental results allows us to assign the ground state structures. A new bent Au–Au–H structure for the ground state of Au_2H is suggested. In addition, we report and discuss the energy-dependent photoelectron anisotropy parameters.

II. EXPERIMENTAL AND COMPUTATIONAL METHODS

The experiments were carried out using our collinear velocity-map photoelectron imaging analyzer with a laser vaporization source. The apparatus has been described in detail elsewhere.¹⁵ Briefly, gold hydrides were generated by laser

^{a)}Authors to whom correspondence should be addressed. Tel.: +86-411-84379365. FAX: +86-411-84675584.

^{b)}Electronic mail: zctang@dicp.ac.cn

^{c)}Electronic mail: fanhj@dicp.ac.cn

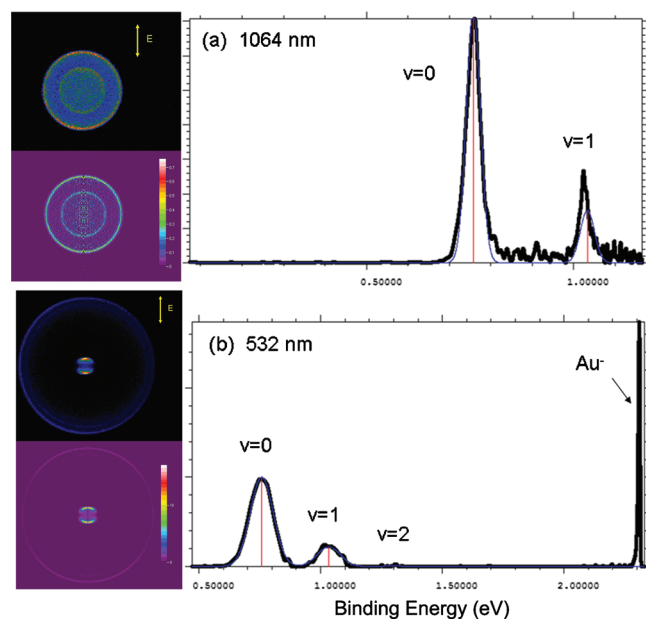


FIG. 1. Photoelectron raw images (top on the left), reconstructed images (bottom on the left), and the photoelectron spectra of AuH^- obtained at (a) 1064 nm (1.165 eV) and (b) 532 nm (2.331 eV). Laser polarization is vertical in the plane of the page. The black lines are the experimental data, and overlapped with the spectra are the FC simulation of the peaks in red.

vaporization of pure gold target. A small amount of methanol molecules (analytically pure) without additional purification were seeded in helium (99.9%) by bubbling the He noble carrier gas through the methanol liquid at room temperature (about 300 K). The negative clusters are extracted perpendicularly from the beam by a -1.2 kV high voltage pulse and are subjected to a McLaren–Wiley TOF mass spectrometer.¹⁶ Then, the anions were introduced into the laser detachment region and interacted with the laser beam from a Nd:YAG (YAG denotes yttrium aluminum garnet) laser: 1064, 532, and 355 nm. The laser propagates perpendicularly to the anion beam axis, with a polarization vector parallel to the imaging plane. The photoelectrons in the detachment region were extracted by a modified collinear VMI electrodes based on the original design of Eppink and Parker.¹⁷ After passing through a 36 cm TOF tube, the photoelectrons mapped onto a detector consisting of a 40-mm-diam microchannel plate assembly and a phosphor screen. The two-dimensional (2D) images on the phosphor screen were recorded by a CCD camera. The photoelectron imaging of Au^- at 355 nm was used for the spectrometer calibration. All the photoelectron images were reconstructed using the basis set expansion (BASEX) inverse Abel transform method,¹⁸ which yielded both the photoelectron spectra and PAD. Generally, each image is accumulated with between 50 000 and 100 000 laser shots at 10 Hz repetition rate. The energy resolution is better than 50 meV at electron kinetic energy (eKE) of 1 eV.

Theoretical studies on UCCSD(T) level were carried out to elucidate the geometric and electronic structures of the neutral and anionic Au_nH ($n=1,2$). Geometric optimizations were performed using aug-cc-pVTZ-pp (Ref. 19) basis sets for Au and aug-cc-pVTZ (Ref. 20) basis sets for H. Frequency calculations on the same level have been done to get

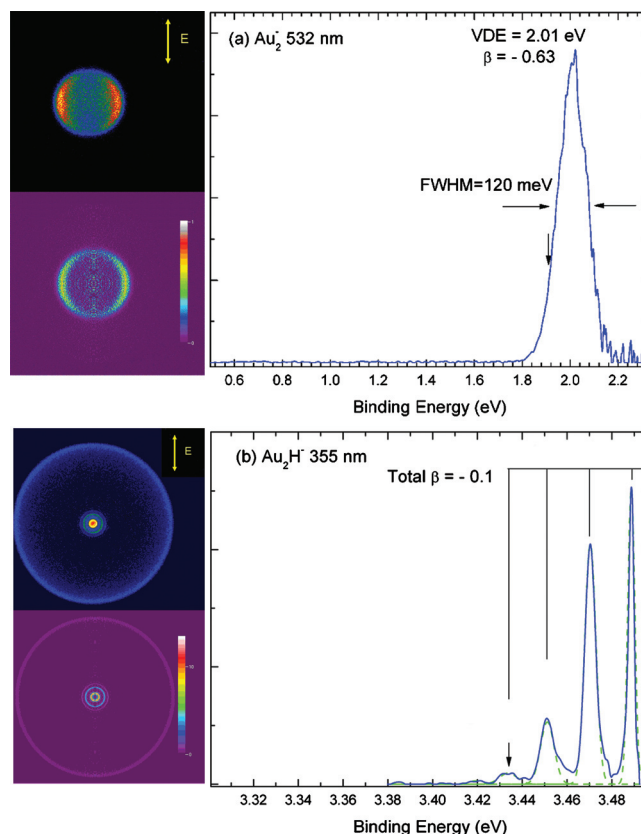


FIG. 2. Photoelectron raw images (top on the left), reconstructed images (bottom on the left), and the photoelectron spectra for (a) Au_2^- obtained at 532 nm (2.331 eV) and (b) Au_2H^- , recorded at 355 nm (3.496 eV). Laser polarization is vertical in the plane of the page. Anisotropy parameters β were determined for the angular distributions.

the zero-point energy and to validate whether the optimized geometries are the true minima. Additional single point calculations have been performed on the optimized geometries. The EAs were computed via the enthalpy difference ($E_{\text{UCCSD(T)}} + \text{ZPE}$) between neutral and anionic states. All calculations have been done by MOLPRO program.²¹

III. RESULTS AND DISCUSSION

The photoelectron images from the detachment of AuH^- and Au_2H^- anions are shown in Figs. 1 and 2, respectively. The raw image (top on the left) collected in the experiments shows the projection of the three-dimensional (3D) laboratory frame photoelectron probability density onto the plane of the imaging detector, and the reconstructed image (bottom on the left) represents the central slice of the 3D distribution from its 2D projection. The laser polarization is vertical in the image plane (double yellow arrow). Photoelectron spectra and the PADs are obtained by integrating the reconstructed images, considering the Jacobian factors. The photoelectron spectra are plotted versus electron binding energy (eBE) $= h\nu - \text{eKE}$. *Ab initio* calculations were performed to elucidate the geometric and electronic structures of the neutral and anionic Au_nH ($n=1,2$). The optimized structures for the neutral and anionic Au_nH ($n=1,2$) are depicted in Fig. 3, and the calculated EAs and vibrational frequencies are summarized in Table I.

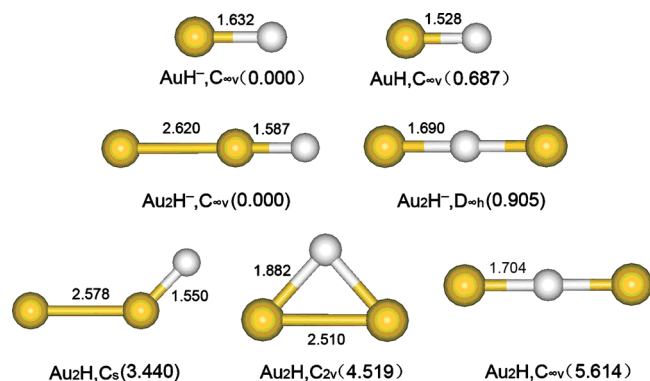


FIG. 3. Optimized ground state structures and low-lying isomers of AuH, AuH⁻, Au₂H, and Au₂H⁻. Bond lengths in Å are given above the bond, and the relative enthalpy ($E_{\text{CCSD}} + \text{ZPE}$) to the anion ground state are given in parentheses in eV.

The experimental results obtained at 1064 nm (1.165 eV) and 532 nm (2.331 eV) for AuH⁻ are shown in Fig. 1. The 1064 nm photoelectron images of AuH⁻ are shown in Fig. 1(a). Two narrow peaks are observed, corresponding to $v=0$ and 1 of the ground state of AuH. The 532 nm photoelectron spectrum in Fig. 1(b) shows four peaks. The former three peaks come from the photodetachment of AuH⁻, while the peak located at 2.309(1) eV comes from the detachment of Au⁻. The former three peaks are transitions from the anionic ground state to the $v=0$, 1, and 2 levels of the ground state of AuH, respectively. This vibration is assigned to the Au–H stretching.^{5,12} For the well-resolved spectrum, the adiabatic EA is defined by the 0-0 original transition of the ground state. Both the EA and VDE are estimated to be 0.758(20) eV. This value agrees with the calculated EA for AuH, which is 0.687 eV.

The short vibrational progression in Fig. 1 allows the use of the Franck–Condon (FC) simulation by the program PESCAL.²² The anionic and neutral electronic ground states were modeled as Morse oscillators. The neutral parameters ($r_e=1.524$ Å, $\omega=2305$ cm⁻¹, and $\omega_e\chi_e=43$ cm⁻¹) were fixed.²³ Due to the lack of vibrational hotbands, only the anionic equilibrium bond length of AuH⁻ was obtained to be 1.597(6) Å. The difference between the anionic ground state and that of the neutral (0.073 Å) is in reasonable agreement with the short vibrational progression. CCSD(T) calculations show $r_e=1.632$ Å for AuH⁻ and $r_e=1.528$ Å for AuH, and predict a longer equilibrium bond length for the anion than for the neutral. The EA is found to be 0.758 eV. The adia-

batic dissociation energy (D_0) of AuH⁻ to Au⁻+H can be obtained from a thermodynamic cycle,

$$D_0(\text{Au}^- - \text{H}) = D_0(\text{AuH}) - \text{EA}(\text{Au}^-) + \text{EA}(\text{AuH}). \quad (1)$$

Utilizing $D_0(\text{AuH})=3.36$ eV,²⁴ the $D_0(\text{AuH}^-)$ is obtained to be about 1.127 eV. Similar to CuH,²⁵ the weaker anionic bond accords with the antibonding character of the added electron.

Previous studies supported that the vertical detachment energies from the doublet anion to the singlet and triplet states of the neutral AuH lied at 0.84 and 3.78 eV, respectively, and a band at 2.1 eV observed in earlier photoelectron spectra could not be assigned based on theoretical calculations.³ More striking, the peak located at 2.1 eV disappears in our experiments [Fig. 1(b)], and the second peak should be located at above 2.33 eV. Our experimental results are in excellent agreement with the previous theoretical results. To confirm the results, the excitation energies of AuH were calculated by EOM-CCSD method²⁶ using aug-cc-pVQZ-pp basis sets for Au and aug-cc-pVQZ basis sets for H. For the first two excited states, we got the excitation energies of 3.850 and 4.920 eV, respectively. Thus, we suggest that the band at 2.1 eV in the former spectrum is a contamination to the single-photon photodetachment of AuH⁻. Moreover, with respect to the bare Au atom [2.309(1) eV], H chemisorption induces a strong decrease of adiabatic electronic affinity of AuH⁻ to 0.758(20) eV.

The photoelectron image results of Au₂⁻ and Au₂H⁻ are displayed in Fig. 2. Figure 2(a) shows the photoelectron images and photoelectron spectrum of Au₂⁻ recorded at 532 nm. Only one peak located at 2.010(20) eV is observed, which corresponds to the Au₂ X ¹Σ_g⁺ ← Au₂⁻ X ²Σ_u⁺ transition from the anionic electronic ground state into the neutral electronic ground state.²⁷ Due to lack of vibrational resolution, the EA of Au₂ is determined approximately by drawing a straight line at the front edge of the peak and then adding an instrumental resolution constant to the intercept with the binding energy axis. The EA value [1.930(20) eV] agrees with the reported EA of 1.938(7) eV.²⁸ The full width at half maximum (FWHM) is about 120 meV, in accordance with composing of 15 vibrational transitions.²⁸ The broad width of the band is confirmed by the reported anion bond length 0.110(7) Å longer than that of the neutral ground state.²⁸

The images and the photoelectron spectrum of Au₂H⁻ at 355 nm (3.496 eV) are displayed in Fig. 2(b). The outside ring is due to contamination of Au₂⁻, as a result of a near

TABLE I. Calculated and experimental EAs and frequencies of the ground state AuH and Au₂H. [The experimental errors are determined by our instrumental resolution ($\Delta E = eKE \times 0.05$).]

	EA (eV)		Au–H vibrational frequency (cm ⁻¹)		Au–Au frequency (cm ⁻¹)	
	Expt.	Calc.	Expt.	Calc.	Expt.	Calc.
AuH	0.758(20)	0.687	2305 ^a	2264		
Au ₂ H	3.437(3)	3.440	2050(100) ^b	2146	148(4)	139

^aReference 23.

^bReference 7.

mass degeneracy between Au_2^- (mass 394) and Au_2H^- (mass 395). Four intense peaks between 3.43 and 3.49 eV [right in Fig. 2(b)] are clearly resolved, which can be assigned to the transition from the anion electronic ground state to the neutral electronic ground state of Au_2H . The EA of Au_2H is measured to be 3.437(3) eV. The photon energy (3.496 eV) is insufficient to access the whole transition from the anion ground state to the neutral ground state, even the vertical detachment energy [3.570(20) eV]⁷ cannot be obtained from the data. Thus, we cannot quantitatively simulate the spectrum. The spectrum of Au_2H^- is dominated by a progression of intense peaks with the average energy spacing of 148(4) cm^{-1} (19 meV). Furthermore, according to the frequency analysis, the small vibrational spacing can be assigned to the Au–Au stretching mode.²⁸ The experimental value (148(4) cm^{-1}) agrees well with the theoretical value of 139 cm^{-1} . To the best of our knowledge, this is the first experimental determination of Au–Au stretching vibrational frequency of Au_2H in the gas phase.

Previous DFT calculations suggested that neutral Au_2H has a triangular structure (C_{2v}), which is very different from the linear structures ($C_{\infty v}$) for Au_2H^- anion.^{4,7} Our CCSD(T) calculations also support that the ground state structure of the Au_2H^- is linear [Au–Au–H]. Another linear isomer, with the structure [Au–H–Au], was found to be 0.905 eV higher in energy than the ground state structure. For neutral Au_2H , the linear [Au–H–Au] structure is still a minimum, like the previous DFT study,⁷ we also observed two imaginary frequencies for the linear [Au–Au–H] structure. On an effort to achieve the true minimum following the vibrational mode of the imaginary frequencies, we located a true minimum with bent Au–Au–H (Au–Au–H = 131°). This isomer is lower in energy than linear [Au–H–Au] by 2.174 eV and turned out to be the ground state structure for neutral Au_2H . To the best of our knowledge, this structure has not been addressed before. In addition, we located another isomer with bridged hydrogen and C_{2v} symmetry. This isomer lies 1.079 eV above the ground state. The calculated EA for Au_2H is 3.440 eV, which is in excellent agreement with the experimental observed value of 3.437(3) eV. This determination of EA(Au_2H) allows us to estimate the anion dissociation energy from a thermochemical cycle, then $D_0(\text{Au}_2^- - \text{H}) - D_0(\text{Au}_2\text{H})$ is 1.497(20) eV. This bond in the anion is much stronger than that in the neutral.

In general, the larger the change in the geometry, the greater the number of vibrational states contributing to the FC progression. The relative populations of the intense four vibrational peaks of Au–Au stretching increase. The extended vibrational progression agrees with the difference (0.042 Å) in the calculated Au–Au bond length between the anion and the neutral. The calculated bending frequency is 280 cm^{-1} . There is a large Au–Au–H angle difference (49°) between the bent neutral and the linear anion. Due to the limited photon energy and the absence of signal at the origin, we have not observed the bending vibrational progression. However, the extended bending progression is expected and is observed above this photon energy.

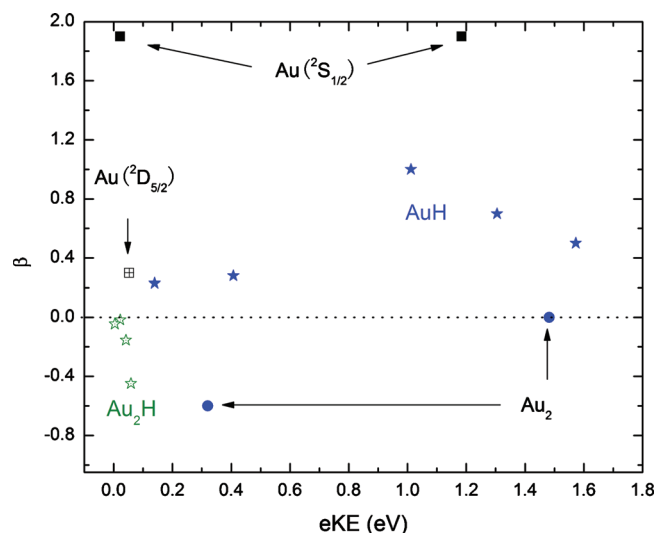


FIG. 4. The anisotropy parameters β vs eKE for Au^- ($^2S_{1/2}$ feature, solid squares, Ref. 15), Au^- ($^2D_{5/2}$ feature, open square), Au_2^- (blue solid circles), AuH^- (blue solid stars), and Au_2H^- (green open stars).

The photoelectron anisotropy parameter (β) from photo-detachment by linearly polarized light can be determined by fitting the function²⁹

$$I(\theta) \propto 1 + \beta P_2(\cos \theta) \quad (2)$$

to the angular distributions derived from the reconstructed images. The anisotropy parameter (β) is between -1 and $+2$, corresponding to perfectly perpendicular and perfectly parallel distributions, respectively. The photoelectron anisotropy parameter (β) contains the information of the molecular orbitals from which the photoelectrons come from and the dynamics of the photoelectron emission events.^{14,30}

Because the images of AuH^- and Au_2H^- show well-resolved vibrational structures, we can obtain the anisotropy parameters of vibrational structures. All of the anisotropy parameters obtained from images are summarized as a function of eKE in Fig. 4. As expected, the angular distributions show strong variations with photon energy, except the $^2S_{1/2}$ state of Au. A typical example for the removal of one s-type electron is the transition of Au from the anion electronic ground state 1S_0 to the neutral ground state $^2S_{1/2}$ of the neutral Au atom. The photoelectrons of the neutral ground state $^2S_{1/2}$ are ejected purely parallel to the electric vector of the linear light (E) and the experimental values $\beta=1.9$ (in Fig. 4) of the neutral ground state $^2S_{1/2}$ at two eKE values: 355 nm (Ref. 15) and 532 nm. The experimental value ($\beta=1.9$) agrees well with the theoretical value ($\beta=2$). The most interesting observation in the current experiment is that the anisotropy parameter β is near zero in very low eKEs in Fig. 4. Clearly, for these systems, the isotropic distribution dominates near the detachment threshold.³¹

IV. SUMMARY

We have studied the photodetachment of AuH^- and Au_2H^- anions using photoelectron VMI. Vibrationally resolved spectra lead to more accurate EAs and vibrational frequencies for the ground state of the neutral gold hydrides.

The adiabatic EAs of Au_nH⁻ ($n=1-2$) are measured to be 0.758(20) and 3.437(3) eV, respectively. In the case of photodetachment from AuH⁻, FC analyses of the AuH spectrum determined that the equilibrium bond length of the anion ground state is 1.597(6) Å. The present photoelectron spectrum of AuH⁻ at 532 nm excludes the contamination band at 2.10 eV in the earlier photoelectron spectra and is in excellent agreement with the theory results. Meanwhile, the photoelectron images of Au₂H⁻ also show a vibrational progression of 148(4) cm⁻¹ assigned to the Au–Au stretching mode at the ground state. *Ab initio* calculation results are in good agreement with the experimental results. For the ground state of Au₂H, a new bent Au–Au–H structure with an angle of 131° is suggested. Moreover, the anisotropy parameters obtained from the images are reported. We tentatively suggested that for the photoelectrons from atom s-type electron in atom case, the angular distribution parameter is constant and is equal to a value of 2.

ACKNOWLEDGMENTS

This work was supported by the National Natural Science Foundation of China (Grant No. 20773126), the Ministry of Science and Technology of China, and the Chinese Academy of Sciences.

¹H. Ito, T. Saito, T. Miyahara, C. M. Zhong, and M. Sawamura, *Organometallics* **28**, 4829 (2009).

²B. Kiran, X. Li, H. J. Zhai, and L. S. Wang, *J. Chem. Phys.* **125**, 133204 (2006); X. Li, B. Kiran, and L. S. Wang, *J. Phys. Chem. A* **109**, 4366 (2005).

³S. Buckart, G. Gantefor, Y. D. Kim, and P. Jena, *J. Am. Chem. Soc.* **125**, 14205 (2003).

⁴D. Fischer, W. Andreoni, A. Curioni, H. Gronbeck, S. Burkart, and G. Gantefor, *Chem. Phys. Lett.* **361**, 389 (2002).

⁵X. Wang and L. Andrews, *J. Am. Chem. Soc.* **123**, 12899 (2001).

⁶L. Andrews and X. F. Wang, *J. Am. Chem. Soc.* **125**, 11751 (2003).

⁷H. J. Zhai, B. Kiran, and L. S. Wang, *J. Chem. Phys.* **121**, 8231 (2004).

⁸T. Okabayashi, E. Y. Okabayashi, M. Tanimoto, T. Furuya, and S. Saito, *Chem. Phys. Lett.* **422**, 58 (2006).

⁹P. Pyykkö, *Angew. Chem., Int. Ed.* **43**, 4412 (2004); J. M. H. Lo and M. Klobukowski, *Theor. Chem. Acc.* **118**, 607 (2007).

¹⁰C. L. Collins, K. G. Dyall, and H. F. Schaefer, *J. Chem. Phys.* **102**, 2024 (1995); H. A. Witek, T. Nakijima, and K. Hirao, *ibid.* **113**, 8015 (2000).

¹¹J. P. Desclaux and P. Pyykkö, *Chem. Phys. Lett.* **39**, 300 (1976).

¹²C. E. Fellows, M. Rosberg, A. P. C. Campos, R. F. Gutierrez, and C. Amiot, *J. Mol. Spectrosc.* **185**, 420 (1997).

¹³J. Y. Seto, Z. Morbi, F. Charron, S. K. Lee, P. F. Bernath, and R. J. L. Roy, *J. Chem. Phys.* **110**, 11756 (1999).

¹⁴A. Sanov and R. Mabbs, *Int. Rev. Phys. Chem.* **27**, 53 (2008).

¹⁵X. Wu, Z. Qin, H. Xie, and Z. Tang, "Collinear velocity-map photoelectron imaging spectrometer for cluster anions," *Chin. J. Chem. Phys.* (to be published).

¹⁶W. C. Wiley and I. H. McLaren, *Rev. Sci. Instrum.* **26**, 1150 (1955).

¹⁷A. Eppink and D. H. Parker, *Rev. Sci. Instrum.* **68**, 3477 (1997).

¹⁸V. Dribinski, A. Ossadtchi, V. A. Mandelshtam, and H. Reisler, *Rev. Sci. Instrum.* **73**, 2634 (2002).

¹⁹D. Figgen, G. Rauhut, M. Dolg, and H. Stoll, *Chem. Phys.* **311**, 227 (2005); K. A. Peterson and C. Puzzarini, *Theor. Chem. Acc.* **114**, 283 (2005).

²⁰T. H. Dunning, *J. Chem. Phys.* **90**, 1007 (1989).

²¹MOLPRO, a package of *ab initio* programs, H.-J. Werner and P. J. Knowles, version 2006.1, R. Lindh, F. R. Manby, M. Schütz *et al.*

²²K. M. Ervin, PESCAL, FORTRAN program, 2010; K. M. Ervin, T. M. Raymond, G. E. Davico, R. L. Schwartz, S. M. Casey, and W. C. Lineberger, *J. Phys. Chem. A* **105**, 10822 (2001).

²³G. Herzberg, *Molecular Spectra and Molecular Structure*, Constants of Diatomic Molecules Vol. IV (Van Nostrand, New York, 1979).

²⁴E. van Lenthe, E. J. Baerends, and J. G. Snijders, *J. Chem. Phys.* **101**, 9783 (1994).

²⁵R. M. D. Calvi, D. H. Andrews, and W. C. Lineberger, *Chem. Phys. Lett.* **442**, 12 (2007).

²⁶T. Korona and H.-J. Werner, *J. Chem. Phys.* **118**, 3006 (2003).

²⁷H. Handschuh, G. Gantefor, P. S. Bechthold, and W. Eberhardt, *J. Chem. Phys.* **100**, 7093 (1994).

²⁸J. Ho, K. M. Ervin, and W. C. Lineberger, *J. Chem. Phys.* **93**, 6987 (1990).

²⁹J. Cooper and R. N. Zare, *J. Chem. Phys.* **48**, 942 (1968).

³⁰K. L. Reid, *Annu. Rev. Phys. Chem.* **54**, 397 (2003).

³¹E. Surber, R. Mabbs, and A. Sanov, *J. Phys. Chem. A* **107**, 8215 (2003).